

Magnetization and Magnetic Circular Dichroism of $\text{La}_{0.7}\text{Sr}_{0.3}\text{MnO}_3/\text{YSZ}$ Polycrystalline Films

Yu. E. Greben'kova^{a,*}, A. E. Sokolov^a, E. V. Eremin^a, I. S. Edel'man^a, D. A. Marushchenko^a,
V. I. Zaikovskii^b, V. I. Chichkov^c, N. V. Andreev^c, and Ya. M. Mukovskii^c

^a *Kirensky Institute of Physics, Siberian Branch of the Russian Academy of Sciences,
Akademgorodok 50–38, Krasnoyarsk, 660036 Russia*

* e-mail: uliag@iph.krasn.ru

^b *Borshkov Institute of Catalysis, Siberian Branch of the Russian Academy of Sciences,
pr. Akademika Lavrentieva 5, Novosibirsk, 630090 Russia*

^c *National University of Science and Technology "MISIS," Leninskii pr. 4, Moscow, 119049 Russia*

Received September 11, 2012

Abstract—The magnetic and magneto-optical properties as well as the surface morphology and structure of $\text{La}_{0.7}\text{Sr}_{0.3}\text{MnO}_3$ polycrystalline films of different thicknesses have been investigated. It has been shown that films have a rough surface with a characteristic in-plane linear dimension of ~ 30 nm, and crystallites with linear dimensions of 10–20 nm are randomly oriented in the plane. The temperature and field dependences of the magnetization of the films indicate their magnetic inhomogeneity. The magnetic circular dichroism spectra contain a number of bands, one of which at 2.4 eV is explained by the contribution of conduction electrons.

DOI: 10.1134/S1063783413040124

1. INTRODUCTION

Compounds of lanthanum manganites of the $\text{La}_{1-x}\text{A}_x\text{MnO}_3$ type with a perovskite structure are of great interest because, at different degrees of doping with a divalent element (A), the system undergoes a sequence of phase transitions with various types of magnetic, structural, and electronic orderings [1–3]. Manganites in the form of thin-film materials satisfy modern requirements of semiconductor electronics and exhibit the colossal magnetoresistance effect at temperatures close to room temperature in weak magnetic fields. In a number of works [4–6] concerned with the study of manganite film structures with different compositions and different degrees of doping with divalent ions (S^{2+}), much attention has been paid to the magneto-optical effects, because magneto-optics provides important information on the electronic and spin structures of the material. In particular, Yamaguchi et al. [4] and Liu et al. [5] investigated the polar Kerr effect, and Sukhorukov et al. [6] examined the Faraday effect in single-crystal films of the $\text{La}_{0.7}\text{Sr}_{0.3}\text{MnO}_3$ (LSMO) composition. It was found that the hole doping of manganites leads to a substantial transformation of the magneto-optical spectra in the same energy range. The spectra also depend on the thickness of the films [4, 5] and on the technological conditions of their deposition [6]. The nature of the peaks observed in the magneto-optical spectra of LSMO films still remains unclear. Among all the magneto-optical effects, the magnetic circular dichroism

(MCD) is the most informative and convenient phenomenon for measurement, because it has been observed only in absorption bands and, in this case, as a rule, there is no contribution from a nonmagnetic substrate [7]. As far as we know, there is only a single work, i.e., the work by Nath et al. [8], devoted to the study of the MCD in manganites, namely, in LSMO epitaxial thin films deposited on two different substrates. These authors obtained MCD spectra in the energy range 1.5–4.5 eV and traced the temperature dependence of the amplitude of the most intense peak of the MCD, which is centered at 3.3 eV. It was found that the temperature dependence of the effect can differ from the temperature behavior of the magnetization, depending on the substrate type. The present paper is devoted to a detailed investigation of the temperature and spectral dependences of the MCD, as well as the temperature and field dependences of the magnetization of LSMO polycrystalline films. Investigation of polycrystalline films permits us to eliminate possible effects due to stresses generated in epitaxial films because of the incomplete matching of the lattice parameters of the film and the substrate.

2. SAMPLE PREPARATION AND EXPERIMENTAL TECHNIQUE

The $\text{La}_{0.7}\text{Sr}_{0.3}\text{MnO}_3$ films were prepared by magnetron sputtering with a residual pressure of 3×10^{-6} Torr in the chamber before deposition [9, 10]. The total

operating pressure of an Ar + O₂ (4 : 1) mixture was equal to 3×10^{-3} Torr. Substrates were made of single-crystal zirconium oxide stabilized with yttrium (YSZ—PDF No. 82-1241), whose temperature during the deposition was 750°C. Experiments were carried out with two series of samples: (1) samples subjected to preliminary cleaning of the substrate surface with an ion gun (samples nos. 1, 2, 3, and 4 with thicknesses of 30, 80, 90, and 100 nm, respectively) and (2) samples without preliminary treatment of the substrate surface (samples nos. 5, 6, 7, and 8 with thicknesses of 20, 50, 75, and 90 nm, respectively). The thickness of the films was specified by the deposition time and was determined ex-situ by the X-ray fluorescence analysis. According to the phase diagram [1], the LSMO films are ferromagnetic at room temperature (the Curie temperature T_C for the bulk material is 350–360 K).

The surface morphology of the prepared films was examined with a Veeco MultiMode atomic force microscope (AFM). Images of LSMO film fragments were obtained on a JEM-2010 electron microscope operating at an accelerating voltage of 200 kV with a resolution of 0.14 nm. The film was separated from the substrate surface and examined in the transmission geometry. It was assumed that the structure of the film did not significantly change as compared to the initial state.

The magnetization (M) was measured on a Quantum Design PPMS-9 instrument in the temperature range from 5 to 320 K in a magnetic field up to 50 kOe, which was directed parallel and perpendicular to the film surface. The temperature dependences of the magnetization were measured in two modes: (i) the sample was cooled in a magnetic field (FC), and (ii) the sample was cooled in a zero magnetic field (ZFC). The magnetization was measured during heating at the same value of the magnetic field as was used during cooling in the FC mode. The field dependences of the magnetization (hysteresis loops) were obtained at $T = 5$ K.

The absorption spectra were measured on a Shimadzu UV-3600 spectrophotometer at room temperature in the range ~ 1 –6 eV. The MCD was measured using the modulation of the polarization state of a light wave: from the right-hand circular to left-hand circular polarization. When the studied sample exhibited an MCD effect, the absorption coefficients of the light waves, which were right-hand and left-hand circularly polarized with respect to the direction of the magnetic moment of the sample, differed from each other. As a result, the light flux that was transmitted through the sample and then was incident on the photodetector appeared to be modulated in intensity. The MCD was measured as the difference between signals in two opposite directions of the external magnetic field. The measurements were performed in magnetic fields of 3 and 6 kOe, which were directed parallel and perpen-

dicular to the film surface, at temperatures in the range from 90 to 380 K in the energy range 1.0–4.5 eV.

3. RESULTS AND DISCUSSION

3.1. Morphology and Structure of the Films

Figure 1 shows the surface morphology and the size distribution of heterogeneities of the films deposited on substrates subjected to different treatments. It can be seen that the surface of the films is characterized by a roughness of 0.2–0.5 nm in height; in this case, more pronounced heterogeneities are also observed. In the films with preliminary treatment of the substrate surface by an ion gun (Fig. 1b), these heterogeneities reach larger sizes.

The electron microscope images of the film fragments are displayed in Fig. 2, in which we can see well-defined crystallites that have linear dimensions of 10–20 nm and are randomly oriented in the plane. It is also seen that, in some cases, the crystallites are located at different depths and superimposed on each other in two or three layers. Within the crystallites, there is a strict alternation of atomic planes.

3.2. Field and Temperature Dependences of the Magnetization

The magnetization curves of all the studied samples are symmetric hysteresis loops with substantially different values of the saturation field (H_s) for orientations of the external magnetic field parallel and perpendicular to the sample plane. A typical shape of these curves is shown in Fig. 3 for sample no. 8 used as an example: the magnetic field is applied parallel to the film plane H_{\parallel} (Fig. 3a) and normal to the film plane H_{\perp} (Fig. 3b). In the first case, the saturation field is $H_s \sim 1$ kOe, whereas in the second case, it is close to 8 kOe, which indicates a predominantly in-plane magnetic anisotropy in the film. The magnetization curve measured in the normal magnetic field differs from the classical case of in-plane anisotropy by the presence of a hysteresis, even though with a very small value of the coercive force. The magnetization in the saturation field (M_s) is identical for the two directions of the external magnetic field and, for sample no. 8, amounts to 730 emu/cm³. A similar pattern is observed for all the samples under investigation; however, the saturation magnetization M_s depends on the film thickness: the larger is the thickness of the film, the greater is the value of the specific magnetization.

A typical shape of the temperature dependences of the magnetization of the films is shown in Fig. 4a. In general, the curves $M(T)$ for the studied samples correspond to the temperature dependences of the magnetization of bulk materials [11]. As judged from the shape of the magnetization curves, the Curie temperature for a number of samples varies within the range of ~ 300 K. However, for the other samples, an

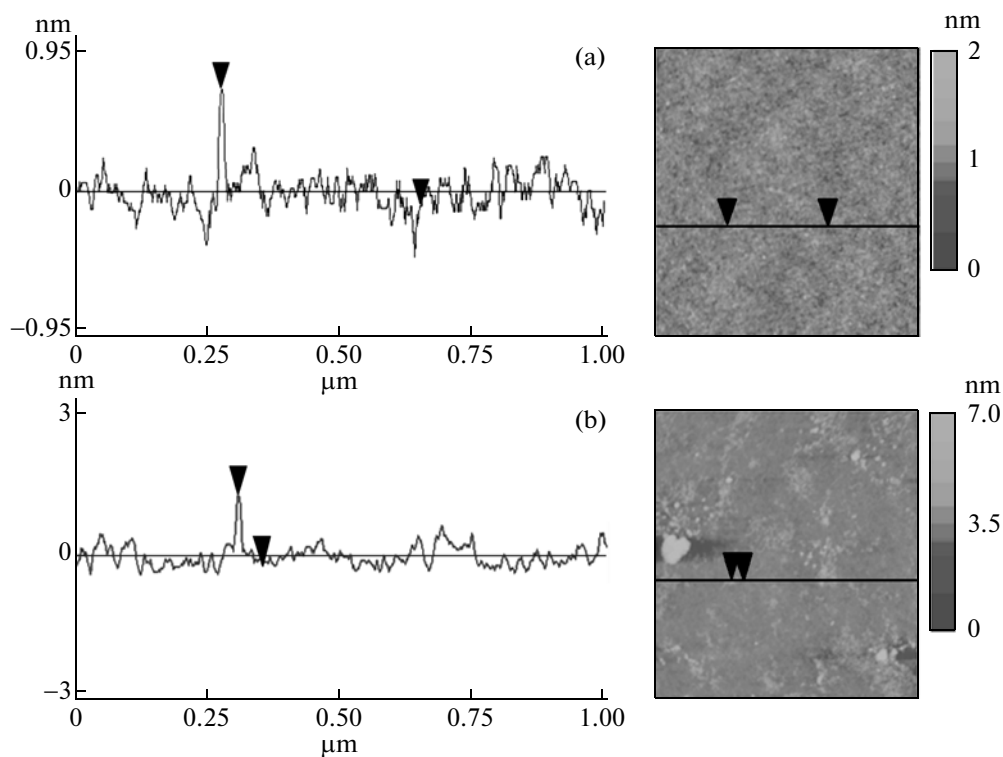


Fig. 1. Surface morphology of films: the top view and the size distribution of heterogeneities in the sample plane for (a) sample no. 6 and (b) sample no. 3.

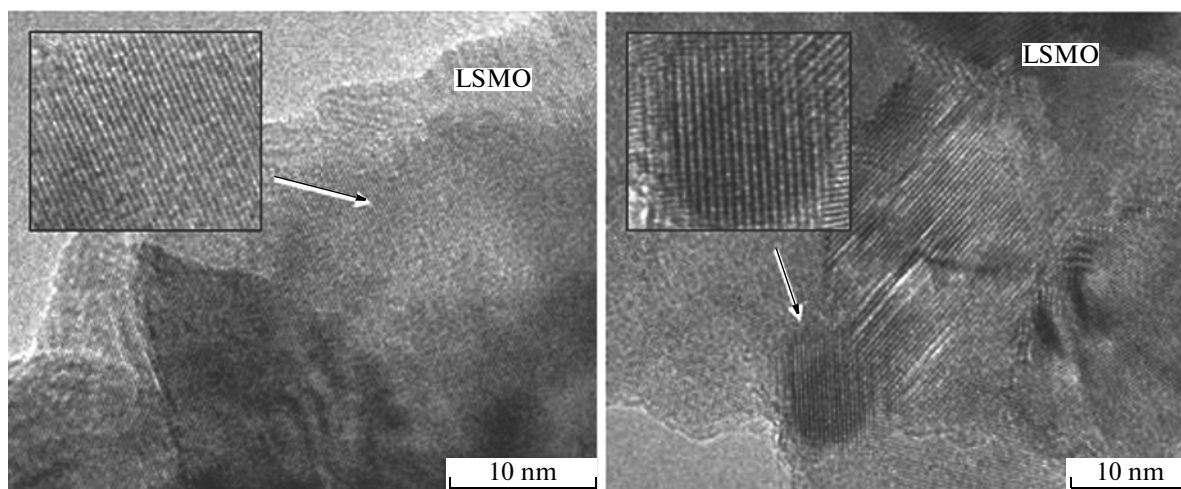


Fig. 2. Electron microscope images of fragments of sample no. 3.

extended tail of the magnetization indicates that, in the bulk of these samples, there are several ferromagnetic regions with different Curie temperatures T_C . This behavior is not related to the treatment of the substrate, because it is observed in both series of samples. The phase heterogeneity most clearly manifests itself in the field dependence of the magnetization of sample no. 2 (Fig. 5a). During the magnetization in the plane of the film, a very narrow hysteresis loop

with a sharply increasing magnetization is observed in weak magnetic fields, a step appears in a magnetic field of ~ 300 Oe, and the complete hysteresis loop is closed in the vicinity of 20 kOe. These patterns are observed in the structures containing layers with different values of the coercivity H_C and the saturation magnetization M_s (see, for example, [12]). In contrast to what is observed in the majority of similar structures, in the case under consideration, this type of the loop is also

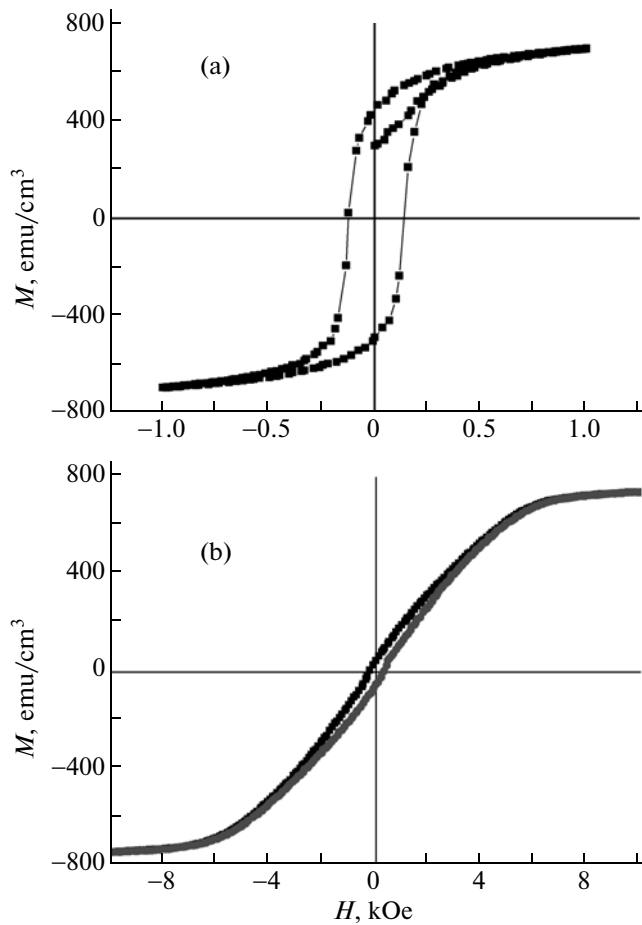


Fig. 3. Field dependences of the magnetization for sample no. 8 at a temperature $T = 5$ K in a magnetic field H directed (a) parallel to the sample surface and (b) perpendicular to the sample surface.

observed in the perpendicular field (Fig. 5b). By comparing the hysteresis loops in the two orientations of the magnetic field, we can assume that two phases coexist in the film: (i) the phase with a predominantly in-plane anisotropy and a small value of the coercivity H_C and (ii) the phase with an anisotropy component perpendicular to the plane and a large value of the coercivity H_C . It is difficult to estimate the total contribution from each of the phases to the magnetization of the sample, because it is determined by both the saturation magnetization M_s and the amount of each phase. What is surprising is the extremely high coercive force of the second phase, which so far has defied explanation.

All the studied films are characterized by the difference between the FC and ZFC temperature dependences of the magnetization obtained in a weak magnetic field $H_{||}$. The ZFC magnetization curve lies below the FC curve and has a maximum. This behavior is shown as an example in Fig. 4b for sample no. 6 and can be explained by a random distribution of the

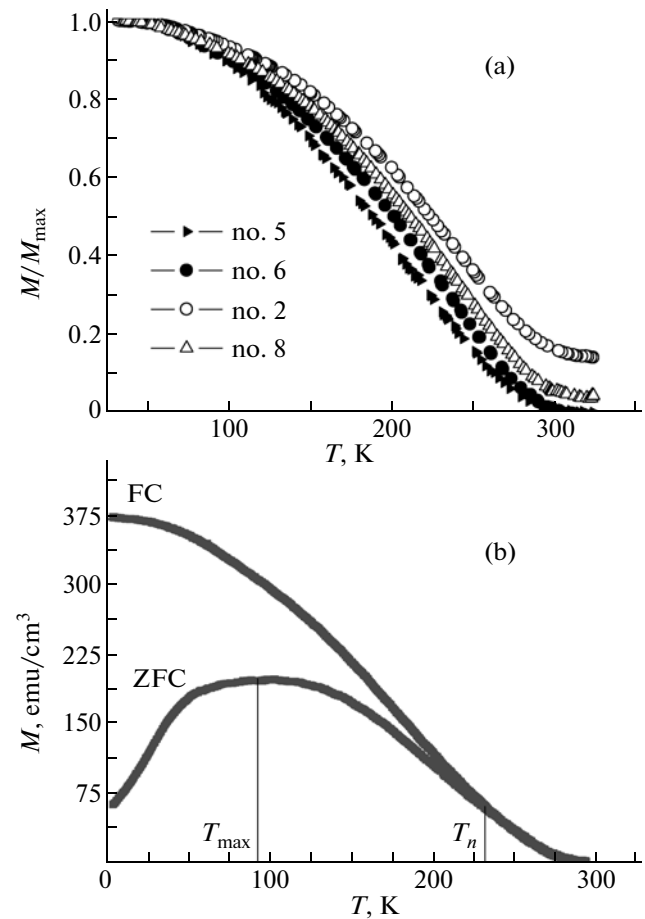


Fig. 4. Temperature dependences of the magnetization in a magnetic field H directed parallel to the sample surface for (a) samples nos. 5, 6, 2, and 8 (film thickness increases in this series) in the FC mode at $H = 1$ kOe; and (b) sample no. 6 in the ZFC and FC modes at $H = 50$ Oe.

easy magnetization axes of the crystallites by analogy with the behavior of magnetically disordered clusters [13]. The irreversibility temperature, at which the ZFC and FC curves diverge, decreases with a decrease in the film thickness.

3.3. Absorption and Magnetic Circular Dichroism

The spectral dependences of the absorption coefficient measured for all samples of two series at room temperature are similar to each other. A typical curve is shown in Fig. 6a. It is characterized by a smooth change in the absorption with an increase of the photon energy and has a broad maximum at ~ 1.5 eV. At the same time, the spectral dependence of the MCD obtained at room temperature in the same energy range exhibits several bands (Fig. 6b). For all the studied samples, the band centered at ~ 1.7 eV is close to the band in the absorption spectrum, and the most intense peak of the MCD is observed at 3.3 eV and agrees with the data presented in [8] (Fig. 6b). It

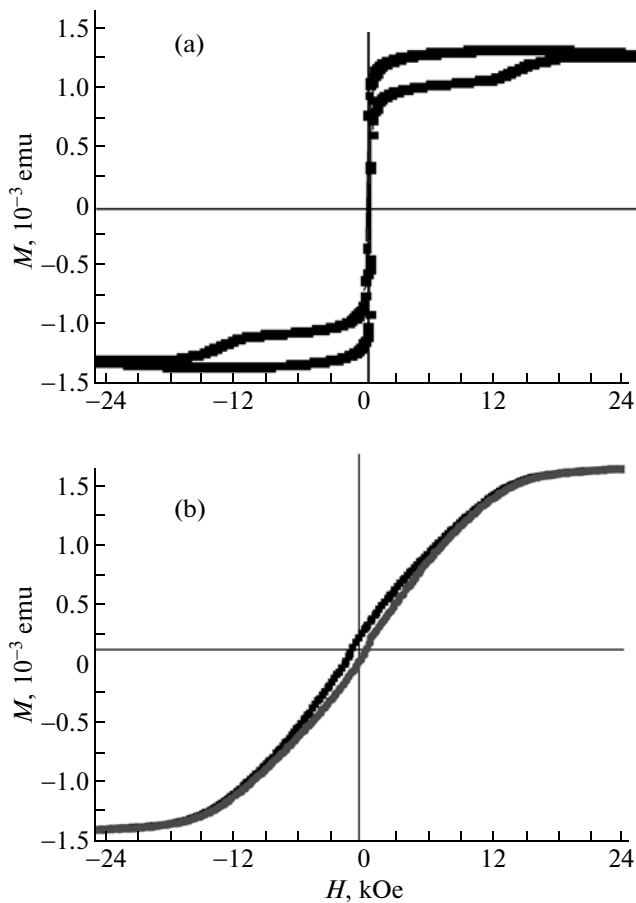


Fig. 5. Field dependences of the magnetization for sample no. 2 at a temperature $T = 5$ K in a magnetic field H directed (a) parallel to the sample surface and (b) perpendicular to the sample surface.

should be noted that the amplitude of this peak, as well as the magnetization, is not proportional to the film thickness (Fig. 6c).

The temperature dependences of the MCD spectra are identical for two series of films with different treatments of the substrate. A typical shape of these dependences is shown in Fig. 7 for samples nos. 2 and 8. It is interesting to note that, in the MCD spectra with a decrease in the temperature, there appears a relatively weak band of opposite sign at approximately 2.4 eV.

In order to determine the nature of the MCD at different energies, the spectra were approximated by Gaussian curves (Fig. 8a). The fitting parameters were as follows: the magnitude of the effect (amplitude), the position of the line, and the line width. The best agreement between the calculated and experimental spectra was achieved under the assumption of four Gaussian bands with energies of 1.7 (13707 cm^{-1}), 2.4 (18860 cm^{-1}), 3.1 (23322 cm^{-1}), and 3.3 (26503 cm^{-1}) eV (curves 1–4 in Fig. 8a, respectively). It was found that the temperature dependences of the band amplitude in Fig. 8b, reduced modulo, differ from each other. The temper-

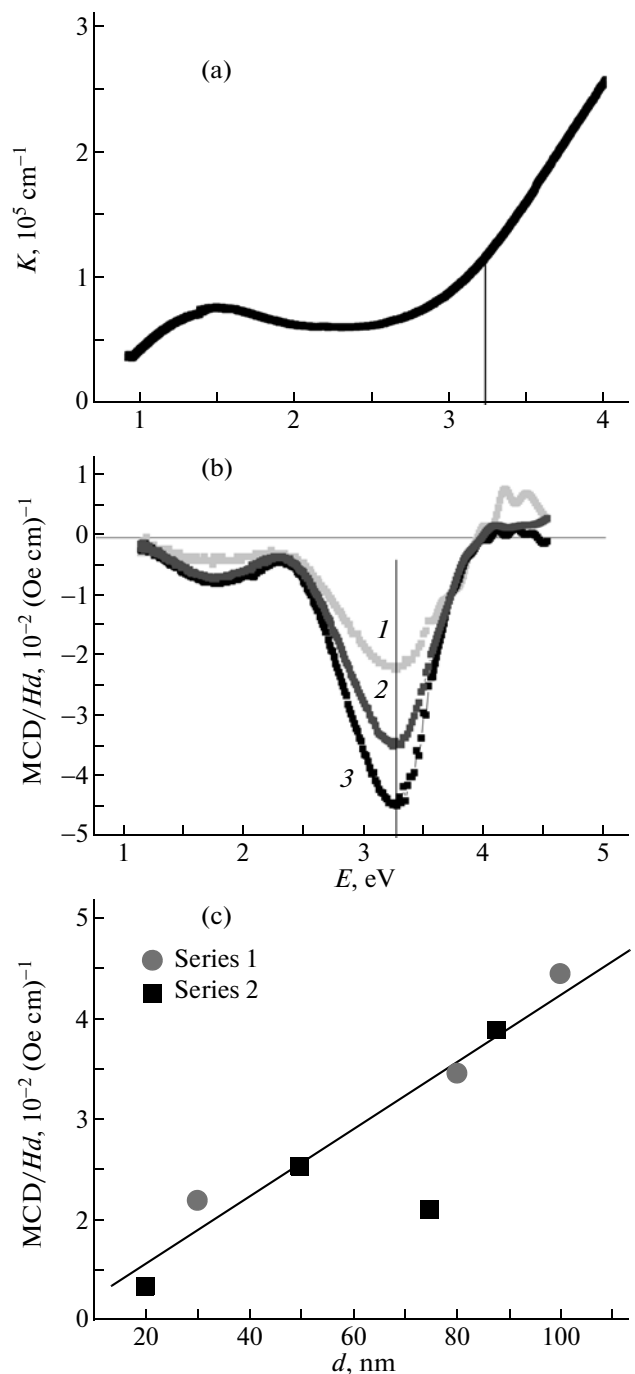


Fig. 6. (a) Absorption spectrum of sample no. 2, (b) spectral dependences of the specific MCD for samples nos. (1) 1, (2) 2, and (3) 4 in a magnetic field H_{\perp} , and (c) dependence of the magnitude of the MCD at 3.3 eV on the thickness of samples of two series. $T = 295$ K.

ature dependences of the band amplitude of the same sign (curves 1, 3, 4) are similar to the temperature dependence of the magnetization for sample no. 8 (curve 5); however, the amplitude of the band with a positive value of the MCD (curve 2) varies according to a different law.

The identical shape of curves 1 and 3–5 indicates that the MCD at the corresponding energies is predominantly determined by the difference in the populations of the sublevels of the ground state of the Mn ions, which is responsible for the magnetization of the sample. Therefore, the MCD described by curves 1, 3, and 4 can correspond to intraionic electronic transitions or charge-transfer transitions between the localized Mn ions, which will be discussed below. The difference in the shapes of curve 2 and the other curves apparently can be associated with a different nature of the MCD.

The observed dependence of the magnetization on the sample thickness can be explained by the disturbance of the magnetic order at the LSMO/YSZ interface, i.e., by the formation of an interface that exhibits other magnetic properties, as was proposed in [14, 15] for the explanation of the specific features of the tunneling in the LSMO–insulator–LSMO heterostructures. The formation of an interface decreases the total magnetization of the sample. The depth of the interface is independent or weakly dependent on the thickness of the film; therefore, the influence of the interface on the magnetic and magneto-optical properties is the weaker, the larger is the thickness of the film.

The difference in the ZFC and FC curves can be explained by the presence of randomly oriented crystallites in the structure of the sample (Fig. 2). When the sample is cooled in a zero magnetic field, the magnetization vector of each crystallite is oriented along the easy magnetization axis of this crystallite, and the total magnetization of the sample is close to zero. Application of a magnetic field during the heating of the sample leads to a gradual alignment of the crystallite magnetic moments along the direction of the field, and at an irreversibility temperature, the FC and ZFC curves merge. The width of the maximum in the ZFC curve is determined by the spread in values of the crystallite characteristics, such as sizes, anisotropies, orientations of easy magnetization axes, and stresses at interfaces. This pattern, as was noted earlier, was observed in [13] and has been explained by the magnetic disorder of clusters.

As was noted above, the spectral dependence of the MCD in the energy range from 1.0 to 3.5 eV exhibits four bands due to the different electronic transitions. The maximum at ~ 1.7 eV (Fig. 6b) is close in energy to the absorption maximum (~ 1.5 eV, Fig. 6a), whose position, in turn, is consistent with the position of the low-frequency absorption band observed in [16]. The nature of this peak was discussed by different authors and assigned to both the $d-d$ transitions and the transitions associated with the O $2p$ –Mn $3d$ charge transfer. In particular, in [6], this maximum was assigned to the spin-allowed $d-d$ transition ${}^5E_g-{}^5T_{2g}$ in the Mn^{3+} ions. The other electronic transitions identified by analyzing the spectral dependence of the MCD of the LSMO film also have a number of different interpreta-

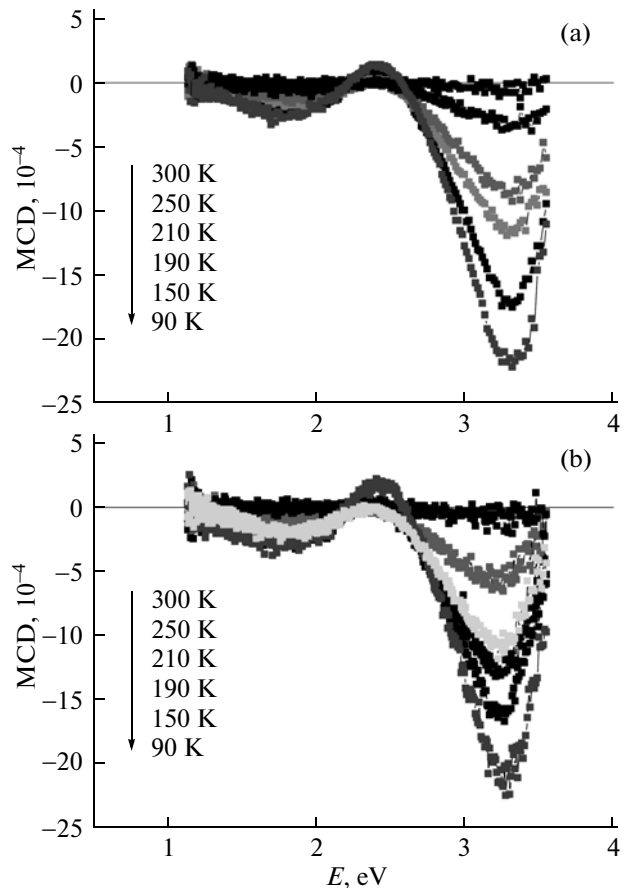


Fig. 7. MCD spectra at different temperatures in a magnetic field $H_{\parallel} = 3$ kOe for samples nos. (a) 2 and (b) 8.

tions. However, the hole doping of $LaMnO_3$, which actually takes place in $La_{0.7}Sr_{0.3}MnO_3$, leads to a substantial transformation of the optical spectrum of the sample. The band intensity can change, whereas the bands themselves can shift toward lower or higher energies. Another consequence of this doping is the formation of octahedral complexes $(MnO_6)^{8-}$. The magneto-optics of $(Mn^{4+}O_6)^{8-}$ complexes was studied in [17] for the $A_2Mn_2O_7$ pyrochlore used as an example. Using the Kerr effect, the authors identified bands near 2.6 and 3.1 eV, which were attributed to the $d-d$ transitions ${}^4A_{2g}-{}^4T_{2g}$ and ${}^4A_{2g}-{}^4T_{1g}$ in the Mn^{4+} ions. Based on the results obtained in [17], the authors of [6] related the asymmetric shape of the peak in the Faraday rotation spectrum to the proximity of the two $d-d$ transitions in the Mn^{4+} ions with different intensities centered at 2.7 and 3.1 eV. As can be seen from Fig. 7, the peak with a maximum at 3.3 eV in the MCD spectrum also has an asymmetric shape. The decomposition of this spectrum into components actually revealed a peak at 3.1 eV, which can be described by a transition associated with Mn^{4+} . As regards the peak centered at 3.3 eV, it should be noted that its amplitude

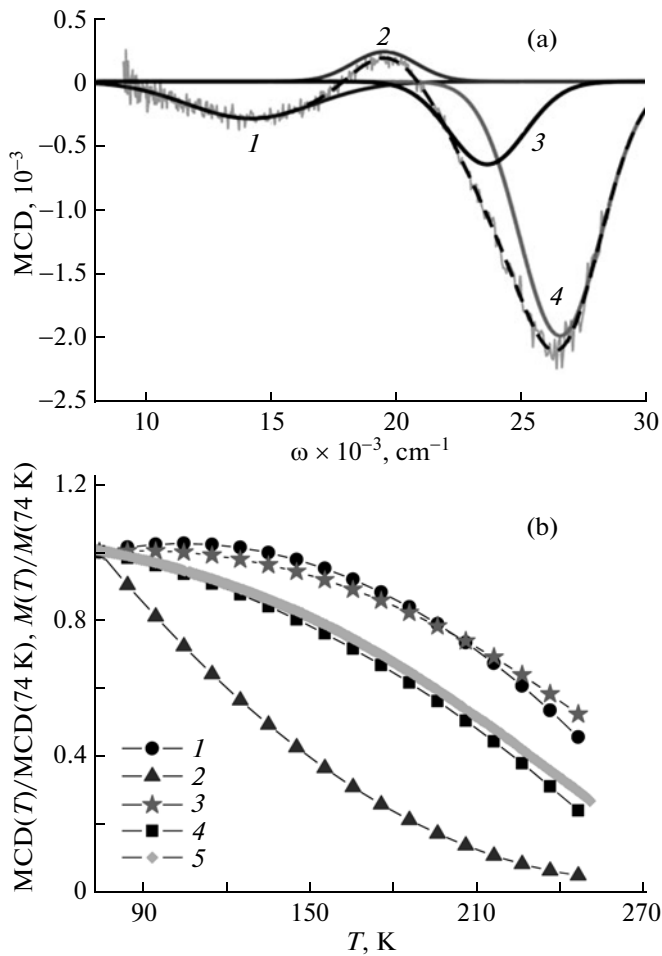


Fig. 8. (a) Approximation of the experimental MCD spectra by Gaussian curves and (b) temperature dependences of (1–4) the amplitudes of four MCD bands and (5) the magnetization in a magnetic field $H_{\parallel} = 3$ kOe for sample no. 8.

is significantly larger than the others. This behavior indicates that the nature of the transition differs from the nature of the low-energy bands. The majority of the authors have attributed this transition to the O $2p$ –Mn $3d$ charge transfer. It should also be noted that the shape of the spectral dependence of the MCD for manganites (Fig. 6b) is similar to the shape of the spectrum of the polar Kerr effect [4, 5, 18]. In particular, in [5], the authors identified several bands corresponding to the MCD bands. The maxima in the range of 2.5 and 3.1 eV were assigned to the d – d transitions in the Mn ions, whereas the peak at 3.3 eV was attributed to the charge transfer between oxygen and manganese. However, the interpretation of the spectral dependence of the Kerr effect in terms of electronic transitions is not a trivial task, because the measured Kerr rotation is a complex function of the diagonal and off-diagonal components of the optical conductivity tensor.

A comparison of the band at ~ 1.7 eV identified in the MCD spectrum with the data presented in [18] shows that this band can be attributed to the e_g – e_g transition in the Mn^{3+} ion, because the aforementioned transition is observed in the LaMnO_3 structure, which does not include Mn^{4+} ions. In turn, based on the data presented in [17], the band in the range of 3.1 eV should be assigned to the d – d transition ${}^4A_{2g}$ – ${}^4T_{1g}$ in the Mn^{4+} ions. There is no doubt that the most intense band centered at 3.3 eV is attributed to the O $2p$ –Mn $3d$ charge-transfer transition.

Of the greatest interest in the MCD spectrum is the band at 2.4 eV. A distinctive feature of this band is the temperature dependence of its amplitude (Fig. 8b, curve 2), which does not correspond to the temperature dependence of the magnetization. For the other transitions, the temperature dependence of the MCD corresponds to the dependence $M(T)$. This difference can be explained by the contribution to the MCD from conduction electrons that appear due to doping. In [19], the investigation of optical conductivity spectra revealed that, as the strontium concentration in $\text{La}_{1-x}\text{Sr}_x\text{MnO}_3$ single crystals increases to $x = 0.3$, this contribution becomes dominant. On the other hand, the conduction electrons are spin-polarized in the magnetic field of the ion core, as was shown in [20, 21]. In this case, the degree of spin polarization significantly differs in the depth and on the surface of the sample. The temperature dependence of the magnetization on the LSMO film surface [20, Fig. 4] is similar in shape to curve 2 presented in this paper in Fig. 8b. In turn, the spin polarization of conduction electrons can be affected by both the free surface and the interface between the film and the substrate [22].

4. CONCLUSIONS

We have investigated the magnetic and magneto-optical properties of $\text{La}_{0.7}\text{Sr}_{0.3}\text{MnO}_3/\text{YSZ}$ polycrystalline films of different thicknesses on substrates subjected to different treatments. It has been revealed that the preliminary cleaning of the substrate surface has no significant effect on the properties of the films.

It has been shown that the structure of the studied samples consist of well-defined crystallites that have linear dimensions of 10–20 nm and are randomly oriented in the plane. The magnetic behavior of the samples demonstrates an increase in the specific magnetization with an increase in the film thickness, which is explained by the influence of the interface layer at the LSMO–insulator boundary. The characteristic shape of the temperature and field dependences of the magnetization of the films indicates their magnetic inhomogeneity. The difference between the FC and ZFC temperature dependences of the magnetization in a weak magnetic field and the maximum of the ZFC curve can be associated with the random distribution

of the easy magnetization axes of the crystallites in the bulk of the film.

The magnitude of the MCD, as well as the magnetization, is not proportional to the thickness of the samples. The MCD bands observed over the entire temperature range below T_C are centered at 1.7, 3.1, and 3.3 eV. These bands correspond to the e_g-e_g transitions in the Mn^{3+} ions, the ${}^4A_{2g}-{}^4T_{1g}$ transitions in the Mn^{4+} ions, and the O $2p$ -Mn $3d$ charge-transfer transitions, respectively. For these transitions, the temperature dependence of the amplitudes is in agreement with the temperature dependence of the magnetization of the sample. When the sample is cooled to temperatures below T_C by approximately 100 K, the MCD spectrum exhibits a relatively weak band of opposite sign near 2.4 eV. A distinctive feature of this band is the temperature dependence of its amplitude, which does not correspond to the temperature dependence of the magnetization. This difference can be explained by the contribution to the MCD from conduction electrons with the spin polarization affected by both the free surface and the interface between the film and the substrate.

ACKNOWLEDGMENTS

The authors would like to thank A.E. Pestun (National University of Science and Technology "MISIS," Moscow, Russia) for preparing the targets used in our experiments.

This study was supported by the Russian Foundation for Basic Research (project nos. 11-02-00972 and 12-02-92607).

REFERENCES

- O. Chmaissem, B. Dabrowski, S. Kolesnik, J. Mais, J. Jorgensen, and S. Short, *Phys. Rev. B: Condens. Matter* **67**, 094431 (2003).
- Ya. M. Mukovskii, *Russ. Khim. Zh.* **45** (5–6), 32 (2001).
- A. Yu. Izyumov and Yu. N. Skryabin, *Phys.—Usp.* **44** (2), 109 (2001).
- S. Yamaguchi, Y. Okimoto, K. Ishibashi, and Y. Tokura, *Phys. Rev. B: Condens. Matter* **58** (11), 6862 (1998).
- H. L. Liu, K. S. Lu, M. X. Kuo, L. Uba, S. Uba, L. M. Wang, and H.-T. Jeng, *J. Appl. Phys.* **99** (4), 043908 (2006).
- Yu. P. Sukhorukov, A. M. Moskvina, N. N. Loshkareva, I. B. Smolyak, V. E. Arkhipov, Ya. M. Mukovskii, and A. V. Shmatok, *Tech. Phys.* **46** (6), 778 (2001).
- A. D. Buckingham and P. J. Stephens, *Annu. Rev. Phys. Chem.* **17**, 399 (1966).
- T. K. Nath, J. R. Neal, and G. A. Gehring, *J. Appl. Phys.* **105** (7), 07D709 (2009).
- E. A. Antonova, V. L. Ruzinov, S. Yu. Stark, and V. I. Tchitchkov, *Supercond. Phys. Chem. Technol.* **14** (8), 1624 (1991).
- V. A. Kozlov, Ya. M. Mukovskii, O. M. Urman, and A. V. Shmatok, *Tech. Phys. Lett.* **22** (3), 227 (1996).
- H. Y. Hwang, S.-W. Cheong, N. P. Ong, and B. Batlogg, *Phys. Rev. Lett.* **77**, 2041 (1996).
- J.-M. Liu, Q. Huang, J. Li, C. K. Ong, and Z. G. Liu, *Appl. Phys. A: Mater. Sci. Process.* **69**, S663 (1999).
- K. Dorr, *J. Phys. D: Appl. Phys.* **39**, R125 (2006).
- M. Bibes, Ll. Balcells, S. Valencia, J. Fontcuberta, M. Wojcik, E. Jedryka, and S. Nadolski, *Phys. Rev. Lett.* **87**, 067210 (2001).
- M. Izumi, Y. Ogimoto, Y. Okimoto, T. Manako, P. Ahmet, K. Nakajima, T. Chikyow, M. Kawasaki, and Y. Tokura, *Phys. Rev. B: Condens. Matter* **64**, 064429 (2001).
- N. N. Loshkareva, Yu. P. Sukhorukov, V. E. Arkhipov, S. V. Okatov, S. V. Naumov, I. B. Smolyak, Ya. M. Mukovskii, and A. V. Shmatok, *Phys. Solid State* **41** (3), 426 (1999).
- E. A. Balykina, E. A. Ganshina, G. S. Krinchik, A. Yu. Trifonov, and I. O. Troyanchuk, *J. Magn. Magn. Mater.* **117**, 259 (1992).
- L. Uba, S. Uba, L. P. Germash, L. V. Bekenov, and V. N. Antonov, *Phys. Rev. B: Condens. Matter* **85**, 125124 (2012).
- L. V. Nomerovannaya, A. A. Makhnev, and A. Yu. Rymyantsev, *Phys. Solid State* **41** (8), 1322 (1999).
- J.-H. Park, E. Vescovo, H.-J. Kim, C. Kwon, R. Ramesh, and T. Venkatesan, *Phys. Rev. Lett.* **81** (9), 1953 (1998).
- M. S. Osofsky, B. Nadgorny, R. J. Soulen, Jr, P. Brousard, M. Rubinstein, J. Byers, G. Laprade, Y. M. Mukovskii, D. Shalyatev, and A. Arsenov, *J. Appl. Phys.* **85** (8), 5567 (1999).
- V. Garcia, M. Bibes, A. Barthelemy, M. Bowen, E. Jacquet, J.-P. Contour, and A. Fert, *Phys. Rev. B: Condens. Matter* **69**, 052403 (2004).

Translated by O. Borovik-Romanova